Journal of Materials Chemistry C

Accepted Manuscript

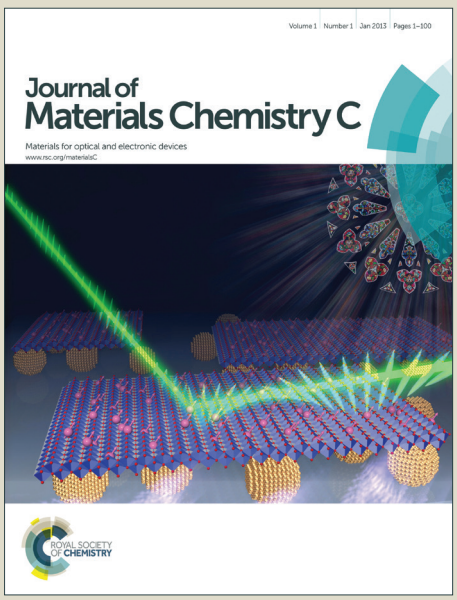

This is an *Accepted Manuscript*, which has been through the Royal Society of Chemistry peer review process and has been accepted for publication.

Accepted Manuscripts are published online shortly after acceptance, before technical editing, formatting and proof reading. Using this free service, authors can make their results available to the community, in citable form, before we publish the edited article. We will replace this *Accepted Manuscript* with the edited and formatted *Advance Article* as soon as it is available.

You can find more information about *Accepted Manuscripts* in the Information for Authors.

Please note that technical editing may introduce minor changes to the text and/or graphics, which may alter content. The journal's standard Terms & Conditions and the Ethical guidelines still apply. In no event shall the Royal Society of Chemistry be held responsible for any errors or omissions in this *Accepted Manuscript* or any consequences arising from the use of any information it contains.

ROYAL SOCIETY OF CHEMISTRY

www.rsc.org/materialsC

Journal of Materials Chemistry C

Dynamic Article Links ►

Cite this: DOI: 10.1039/c0xx00000x

COMMUNICATION

Fabrication of highly electrically conducting fine patterns via substrate-independent inkjet printing of mussel-inspired organic nano-material

Siyuan Ma,[a] Liang Liu,[a] Vadim Bromberg,[a] and Timothy J. Singler*[a]

Received (in XXX, XXX) Xth XXXXXXXXX 20XX, Accepted Xth XXXXXXXXX 20XX

DOI: 10.1039/b000000x

We report the inkjet printing of an aqueous suspension of synthesized mussel-inspired poly(dopamine) nanoparticles. Fine lines of printed nanoparticles were deposited on both glass and polyethylene terephthalate (PET) substrates by exploiting the coffee ring effect. Deposited particles were then used for site-selective silver metallization via a simple electroless plating process at controlled temperature (30°C) and plating time (12min to 120min). The resulting narrow lines of silver exhibited a resistivity 10× that of bulk silver. Lines on PET retained good electrical and adhesion performance even after prolonged bending tests. This technique satisfies general requirements of flexible electronics manufacturing – low temperature, low cost, small feature size and good electrical conductivity independent of substrate material.

Electrically conducting patterns are essential structures for emerging flexible electronics. Drop-on-demand inkjet printing is a material-conservative deposition process compatible with the low temperature requirements of flexible polymer substrates[1]. The implementation of printing within a roll-to-roll (R2R) infrastructure enables continuous, high-speed and large-scale manufacturing. The functional materials suitable for inkjet printing are generally available as nanoparticle (NP) dispersions and precursor solutions[2]. The NP ink is comprised of functional cores surface-coated by a stabilizing agent and uniformly dispersed in a volatile liquid; precursor inks are metal salts dissolved in suitable solvents[2]. To transform printed deposits into a highly electrical conducting phase, a post-printing process is generally required either to remove the adsorbed stabilizing agent and sinter the functional cores (for NP inks) or to precipitate metal structure *in-situ* (for precursor inks)[2]. The standard approach is the application of heat in a controlled ambient environment. The thermal sensitivity of low-cost flexible substrates (such as polyethylene terephthalate (PET)) has led to extensive research into alternative non-thermal techniques such as laser[3], UV[4,5]/IR[6] light, electrical field[7], chemical[8] and plasma[9,10]. However, these post-printing processes generally require sophisticated and expensive equipment. In this letter, we report a printing process for patterned metal deposition which employs site-selective electroless plating (ELP) of silver (Ag) on printed patterns of organic NPs.

Electroless plating generally uses a solution of metal salt, reducing agent, a complexing agent, and additive(s) (such as bath stabilizer and plating rate adjusting agent)[11]. Metal nucleates on the catalytically active surface and continues to promote further metal reduction and growth. This is the defining characteristic of ELP's autocatalytic nature. [11]. A pre-patterned catalyst layer on the target substrate will promote site-selective deposition. Hidber *et al.*[12] utilized microcontact stamping to pattern palladium (Pd) colloids which yielded copper (Cu) patterns after ELP. Harkness *et al.*[13] used photolithography to pattern a Pd-bonded-organic seed layer (hydrogen silsesquioxane) and achieved site selective ELP of Cu and Ag. The prohibitively large cost of photolithography has prompted research into the use of inkjet printing to directly pattern the catalyst[14–20]. Most of the inkjet printing studies exploited Pd-based ink[14–18] while the investigation of other ink materials has been less focused[19,20]. Furthermore, the application of Pd-based inks is limited in versatility because ink-substrate adhesion is substrate dependent[14–20]. Finally, although Pd-based catalyst is useful for electroless plating of a wide range of metals, its high cost prohibits its use for many applications[21].

A mussel-inspired organic polymer poly(dopamine) (PDA) was recently found capable of triggering metal ion reduction[22] leading to its implementation as an ELP catalyst[23,24]. PDA also shows universal adhesion on a wide range of organic and inorganic materials[22]. PDA can be synthesized as either continuous coatings by triggering dopamine polymerization in pure water[22] or as spherical nanoparticles in water-alcohol mixtures at controlled PH[25]. Studies show that polydopamine nanoparticles (PDA-NP) retain the same surface chemistry as continuous PDA coatings[22,25].

Inkjet printing as a method of creating fine features suffers from the limitation of the individual drop size, which can range from 20-80μm[26–29]. We have recently reported a technique that exploits the so-called "coffee-ring" phenomenon studied in sessile drops[30]. In a printed line of dilute particle ink, evaporative deposition of particles at the contact line can produce a pair of parallel lines with minimal solid deposit between the lines[31]. The resulting line widths can be controlled to less than 10% of the

Journal of Materials Chemistry C Accepted Manuscript

printed droplet diameter[30].

In this study, we report a novel patterned metal deposition technique that combines twin line inkjet printing of aqueous PDA nanoparticle ink with site-selective ELP of Ag on both glass and PET substrates. To the best of our knowledge, the inkjet printing of PDA-based nanoparticle ink for patterned metal deposition has not been reported. We report the effect of plating time on morphology, crystalline structure, and electrical resistivity of lines of plated silver. The reliability of Ag lines on flexible PET substrates subjected to cyclic bending and adhesive tape tests is also reported.

Polydopamine nanoparticle (PDA-NP) powder was synthesized according to a published protocol[25]. Briefly, PDA-NPs were generated by initiating dopamine self-polymerization in a water-isopropanol mixture which was buffered by Tris (See ESI†). The average size of PDA-NP was measured with a dynamic light scattering system (Zetasizer-Nano, Malvern) to be 338 ± 55nm (See ESI†). The as-synthesized PDA-NP powder was dispersed in distilled deionized (DI) water at 1 % wt by 10min agitation by ultra-sonication. The viscosity and surface tension of the PDA-NP ink were measured as 1.0± 0.1 mPas and 72.3± 0.1 mNm^{-1} using a cone-plate rheometer (AR1000, Texas Instrument) and bubble pressure tensiometer (BP100, Kruss), respectively

A single-nozzle inkjet printer was used to print the PDA-NP suspension onto plasma-treated glass substrates (2947, Corning) and PET substrates (Melinex ST506, Dupont) to form arrays of five lines (Scheme 1 and ESI†). Evaporative-driven transport in the presence of a pinned contact line leads to potential deposition of particles at the contact lines. The result is a twin line particle pattern with minimal interline particle deposition (Fig. 1a and ESI†). Each of the twin lines measured 24 ± 1μm and 10 ± 1μm in width for the glass and PET substrates, respectively.

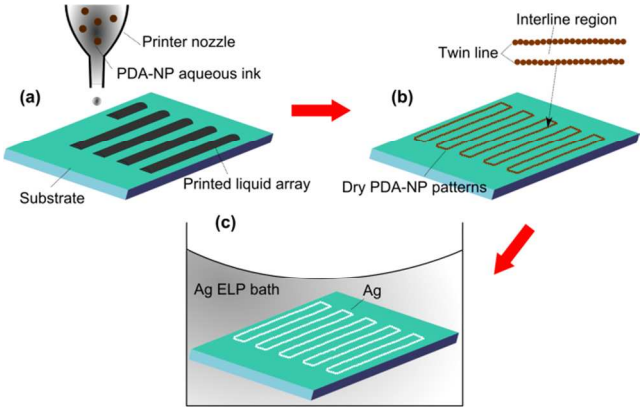

Scheme 1 (a) Poly(dopamine) nanoparticles (PDA-NP) were prepared as aqueous ink and inkjet printed on glass substrate; (b) patterned lines of PDA-NP were formed after evaporation; (c) Ag was site-selectively deposited on PDA-NP patterns after electroless plating

Ag deposition onto the printed pattern can be achieved by simple immersion into a silver salt solution such as silver nitrate ($AgNO_3$)[22]. However, an ELP process that includes an additional reducing agent is necessary to ensure the rapid formation of a continuous and sufficiently thick metal layer. A potential mechanism of PDA-induced ELP has been suggested to involve the electrostatic interaction of metallic ions with surface catechol groups of PDA followed by catechol oxidation to quinone and reduction of metallic ions to elemental metal. The newly deposited elemental metal further catalyzes the redox reaction for continuous deposition. In this study, Ag ELP was performed by immersing the printed PDA patterns in a chemical bath at 30°C for different durations (See ESI†).

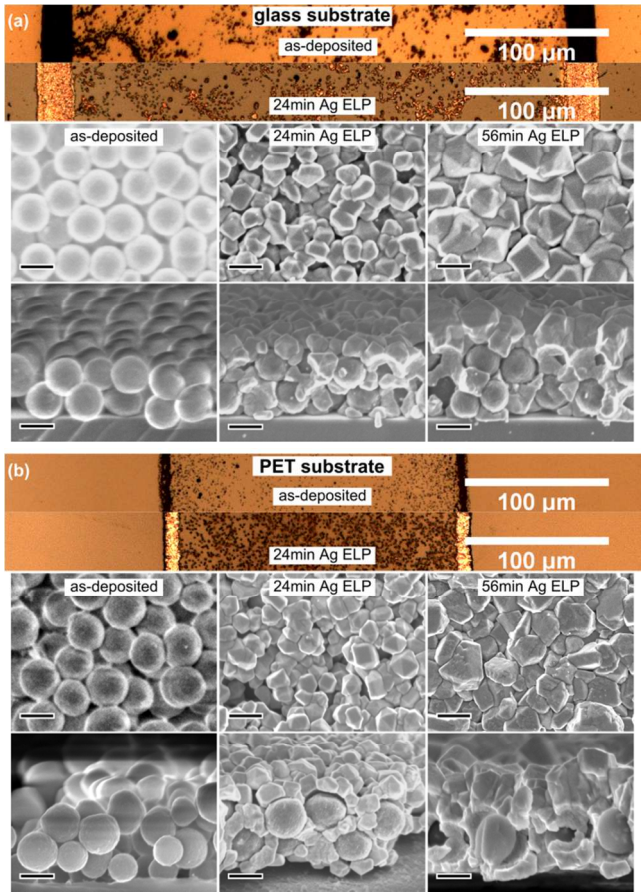

Fig. 1 Typical microscopic images of inkjet printed polydopamine nanoparticle (PDA-NP) twin line regions as a function of silver electroless plating (Ag ELP) time on glass (a) and PET (b) substrates: optical microscopic images, top view and cross-secional view scanning electron microscopic (SEM) images of twin line regions. The SEM image scale bars are 300nm.

The morphology of the printed twin line region before and after the plating process was characterized by optical microscopy (Axio Imager, Zeiss) and scanning electron microscopy (SEM) (Supra 55VP, Zeiss). Top and cross-sectional views show that for the as-deposited lines, each twin line typically consists of a 1-2 particles thick PDA-NP structure (Fig. 1(a,b), SEM). At early time Ag ELP, small Ag grains nucleate on top of each twin line. The grains grow in size and merge to form a slightly granular but continuous Ag layer with extended ELP time. The Ag continuity and grain size increase with extended ELP time. No obvious structural differences in particle deposits on glass and PET substrates were observed. The SEM images of the interline region can be found in the ESI†.

Cross-sectional SEM images were also analyzed to measure the Ag thickness on each twin line as a function of metal plating time (Fig. 2(a)). In general, the Ag growth rate is linear with ELP time and exhibits no apparent differences between glass and PET

Journal of Materials Chemistry C Accepted Manuscript

This journal is © The Royal Society of Chemistry [year]

substrates.

The electrical resistance of Ag-plated lines was measured using a line scratching technique[10,30]. Briefly, a pair of Ag electrodes was sputtered through a mask over each line array so that the lines spanned the distance (4mm) between electrodes (ESI†). Four-point-probe measurements were carried out to determine the total resistance of the five lines. Each line was carefully cut by a needle attached to a micro-positioner and the new resistance value recorded. Under the assumption that each line array is a parallel resistor network, this method allowed measuring the average resistance of each cut line. As Fig. 2(b) shows, single line resistance decreases rapidly within 24min (62Ω and 212Ω for glass and PET, respectively) of ELP, followed by a slower decay on a longer time scale to reach the lowest value of 12Ω for glass and 33Ω for PET at 120min. It was possible to determine whether the Ag in interline region contributed to the measured resistance by disconnecting all the twin lines. It was found that for plating times longer than 58min (glass) and 96min (PET), an electrically conductive path forms in the interline region. However (as Fig. 2(b) shows), this structural transition did not correlate with a measured transition in line resistance, which implies that the resistance of the interline region is much larger than that of each twin line.

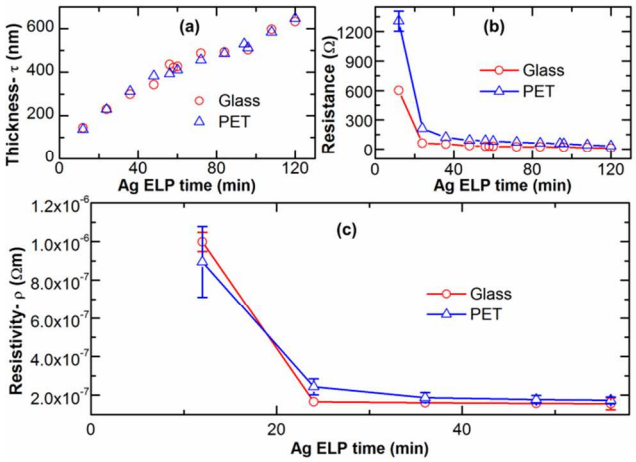

Fig. 2 Deposited structural characterization: (a) thickness (τ) evolution at twin region; (b) individual-line resistance as a function of silver electroless plating time; (c) electrical resistivity change at twin regions from 12min to 56min silver electroless plating.

The electrical resistivity of Ag plated on each twin line was estimated for ELP duration of 56min or shorter, i.e., before the transition to inter-line conductivity on each substrate (see ESI†). A twin-line structure consisting of two parallel conductors with no electrical contribution from the interline region was assumed. The resistivity (ρ) can be expressed as $\rho = 2R\tau W/L$, where R the measured resistance of a twin line, τ the Ag thickness, W the width of each twin line and L the length between two electrodes. Fig 2(c) plots ρ as a function of ELP time forboth glass and PET substrates. At the same Ag ELP time, resistivity is similar for both substrates. Within the first 24min of plating, ρ reaches a value which is about 10.4× and 15.2× larger than the resistivity of bulk Ag, for glass and PET, respectively. After longer plating time, ρ decreases slowly. The lowest values for ρ are 1.57E-7 Ωm (on glass) and 1.74E-7 Ωm (on PET) after 56min Ag ELP which are 9.8× and 10.9× the bulk Ag resistivity, respectively.

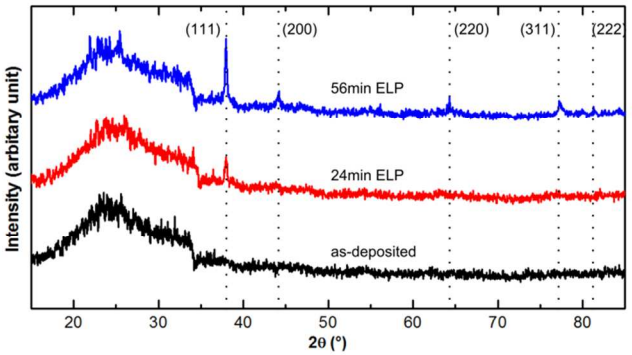

Fig. 3 XRD patterns of the inkjet printed PDA-NP arrays on glass substrates as a function of Ag ELP time: The dotted lines indicate 2θ values of face-centered-cubic Ag according to the Joint Committee on Powder Diffraction Standards (JCPDS) file 04-0783.

The composition of the deposited Ag was confirmed by crystallographic analysis with X-ray diffraction (XRD) (Equinox 2000, Inel) on each array. Ag diffraction patterns after different plating times are shown in Fig. 3. A large diffraction peak around 25° indicates the contribution of the amorphous glass substrate. As-deposited PDA patterns did not display any characteristic diffraction peaks. The appearance of a strong peak at 38.1° after 24min plating indicates Ag (111) crystal planes. After 56min, the peak intensity at 38.1° increases and four additional peaks appear at about 44.1°, 64.4°, 77.3° and 81.4°, corresponding to Ag crystal planes of (200), (220), (311) and (222), respectively. The emergence of characteristic Ag peaks and their increase in intensity is consistent with the appearance and growth of distinct layer observed from SEM.

The mechanical robustness of Ag patterns on PET was assessed using a cyclic bending test. The bending tests were conducted by a cylindrical mandrel bend tester[32]. For each bending cycle, Ag patterns on PET substrates were subjected to both concave and convex geometries alternatively with a 2.5mm radius of curvature (Fig. 4(a)). The tests were conducted at 100 cycles/min frequency in a room environment. The resistance values of each Ag twin line pair which formed by 24min and 56min ELP were measured as a function of bending cycles (Fig. 4 (b)). The results show that electrical resistance begins to increase only after 1000 cycles**.** The increase in resistance after 1000 cycles was correlated with line structure damage observed under SEM after bending tests (ESI†).

Adhesion of the Ag patterns to the substrate was assessed qualitatively using a tape peel test. Adhesive tape (Scotch 600, 3M) was carefully attached to the Ag patterns (24min ELP time on both glass and PET) and subsequently removed (Fig. 4(c)). No change in line structure was observed after the test. Similarly, there was no observable change after tape removal for samples that underwent 6000 bending cycles.

In conclusions, fine lines of Ag with low electrical resistivity were fabricated by sequential inkjet printing of mussel-inspired poly(dopamine) nanoparticle ink and Ag electroless plating. The process yields Ag lines with thickness linearly dependant on plating time and electrical resistivity 10× and 11× that of bulk silver, on glass and PET substrates, respectively. This process demonstrates a simple, low temperature and low-cost method of fabricating fine conductive patterns for flexible electronics applications. The combined approach of inkjet printing organic

Journal of Materials Chemistry C Accepted Manuscript

nano-materials and ELP was reported for the first time.

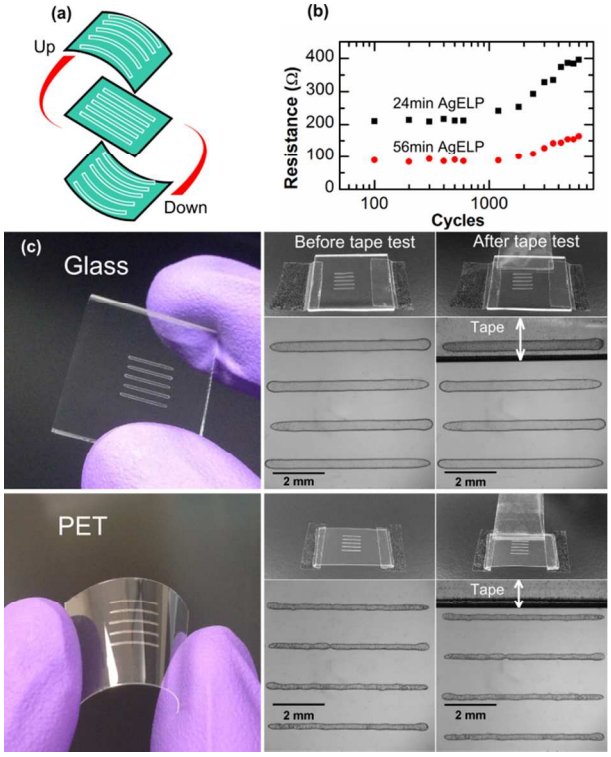

Fig.4 Cyclic bending and adhesion characterization: (a) schematic of each cycle of bending test of the Ag patterns formed on PET substrates; (b) Resistance values of a twin line pair as a function of bending cycles; (c) adhesive tape peeling test of the formed Ag patterns on glass (top row) and PET (bottom row) substrates.

The research was funded by the Analytical and Diagnostics Laboratory (ADL) at Binghamton University's Small Scale Systems Integration and Packaging Center (S3IP).

Notes and references

[a] *Department of Mechanical Engineering, State University of New York (SUNY) at Binghamton, Binghamton, USA. Fax: +01607-777-4620; Tel: +01 607-777-4330; E-mail: singler@binghamton.edu*

† Electronic Supplementary Information (ESI) available: polydopmaine nanopartilce synthesis and size characterization, substrate preparation, inkjet printing apparatus, electroless plating recipe, interline region SEM, electrodes sputtering, resistivity calculations and structural damage after bending test. See DOI: 10.1039/b000000x/

1. A. Teichler, J. Perelaer, and U. S. Schubert, *J. Mater. Chem. C*, 2013, **1**, 1910.
2. J. Perelaer, P. J. Smith, D. Mager, D. Soltman, S. K. Volkman, V. Subramanian, J. G. Korvink, and U. S. Schubert, *J. Mater. Chem.*, 2010, **20**, 8446.
3. S. H. Ko, H. Pan, C. P. Grigoropoulos, C. K. Luscombe, J. M. J. Fréchet, and D. Poulikakos, *Nanotechnology*, 2007, **18**, 345202.
4. A. Solieman, A. H. Moharram, and M. A. Aegerter, *Appl. Surf. Sci.*, 2010, **256**, 1925–1929.
5. J. J. P. Valeton, K. Hermans, C. W. M. Bastiaansen, D. J. Broer, J. Perelaer, U. S. Schubert, G. P. Crawford, and P. J. Smith, *J. Mater. Chem.*, 2010, **20**, 543.
6. D. Tobjörk, H. Aarnio, P. Pulkkinen, R. Bollström, A. Määttänen, P. Ihalainen, T. Mäkelä, J. Peltonen, M. Toivakka, H. Tenhu, and R. Österbacka, *Thin Solid Films*, 2012, **520**, 2949–2955.
7. S. Jang, D. J. Lee, D. Lee, and J. H. Oh, *Thin Solid Films*, 2013, **546**, 157–161.
8. S. Magdassi, M. Grouchko, O. Berezin, and A. Kamyshny, *ACS Nano*, 2010, **4**, 1943–8.
9. I. Reinhold, C. Hendriks, and R. Eckardt, *J. Mater. Chem.*, 2009, **19**, 3384.
10. V. Bromberg, S. Ma, F. D. Egitto, and T. J. Singler, *J. Mater. Chem. C*, 2013.
11. G. O. Mallory and J. B. Hajdu, *Electroless plating: fundamentals and applications*, William Andrew, 1st edn., 1991.
12. P. C. Hidber, W. Helbig, E. Kim, and G. M. Whitesides, *Langmuir*, 1996, **12**, 1375–1380.
13. B. R. Harkness, M. Rudolph, and K. Takeuchi, *Chem. Mater.*, 2002, **14**, 1448–1451.
14. S. W. Suh, J. J. Kim, S. H. Kim, and B. K. Park, *J. Ind. Eng. Chem.*, 2012, **18**, 290–294.
15. S. Busato, A. Belloli, and P. Ermanni, *Sensors Actuators B Chem.*, 2007, **123**, 840–846.
16. P. Shah, Y. Kevrekidis, and J. Benziger, *Langmuir*, 1999, **15**, 1584–1587.
17. C.-C. Tseng, C.-P. Chang, Y. Sung, Y.-C. Chen, and M.-D. Ger, *Colloids Surfaces A Physicochem. Eng. Asp.*, 2009, **339**, 206–210.
18. T. Zhang, X. Wang, T. Li, Q. Guo, and J. Yang, *J. Mater. Chem. C*, 2013.
19. Q. Zhou, H. Chen, and Y. Wang, *Electrochim. Acta*, 2010, **55**, 2542–2549.
20. K. Akamatsu, S. Ikeda, H. Nawafune, and H. Yanagimoto, *J. Am. Chem. Soc.*, 2004, **126**, 10822–3.
21. P. Zhu, Y. Masuda, and K. Koumoto, *J. Mater. Chem.*, 2004, **14**, 976.
22. H. Lee, S. M. Dellatore, W. M. Miller, and P. B. Messersmith, *Science*, 2007, **318**, 426–30.
23. Y. Liao, B. Cao, W.-C. Wang, L. Zhang, D. Wu, and R. Jin, *Appl. Surf. Sci.*, 2009, **255**, 8207–8212.
24. H. Yang, Y. Lan, W. Zhu, W. Li, D. Xu, J. Cui, D. Shen, and G. Li, *J. Mater. Chem.*, 2012, **22**, 16994.
25. J. Yan, L. Yang, M.-F. Lin, J. Ma, X. Lu, and P. S. Lee, *Small*, 2013, **9**, 596–603.
26. J. Doggart, Y. Wu, and S. Zhu, *Appl. Phys. Lett.*, 2009, **94**, 163503.
27. H. Meier, U. Löffelmann, D. Mager, P. J. Smith, and J. G. Korvink, *Phys. status solidi*, 2009, **206**, 1626–1630.
28. B. Derby, *Annu. Rev. Mater. Res.*, 2010, **40**, 395–414.
29. J. Stringer and B. Derby, *J. Eur. Ceram. Soc.*, 2009, **29**, 913–918.
30. V. Bromberg, S. Ma, and T. J. Singler, *Appl. Phys. Lett.*, 2013, **102**, 214101.
31. R. D. Deegan, O. Bakajin, T. F. Dupont, G. Huber, S. R. Nagel, and T. A. Witten, *Nature*, 1997, **389**, 827–829.
32. M. M. Hamasha, K. Alzoubi, S. Lu, and S. B. Desu, *Thin Solid Films*, 2011, **519**, 6033–6038.

Journal of Materials Chemistry C Accepted Manuscript

This journal is © The Royal Society of Chemistry [year]

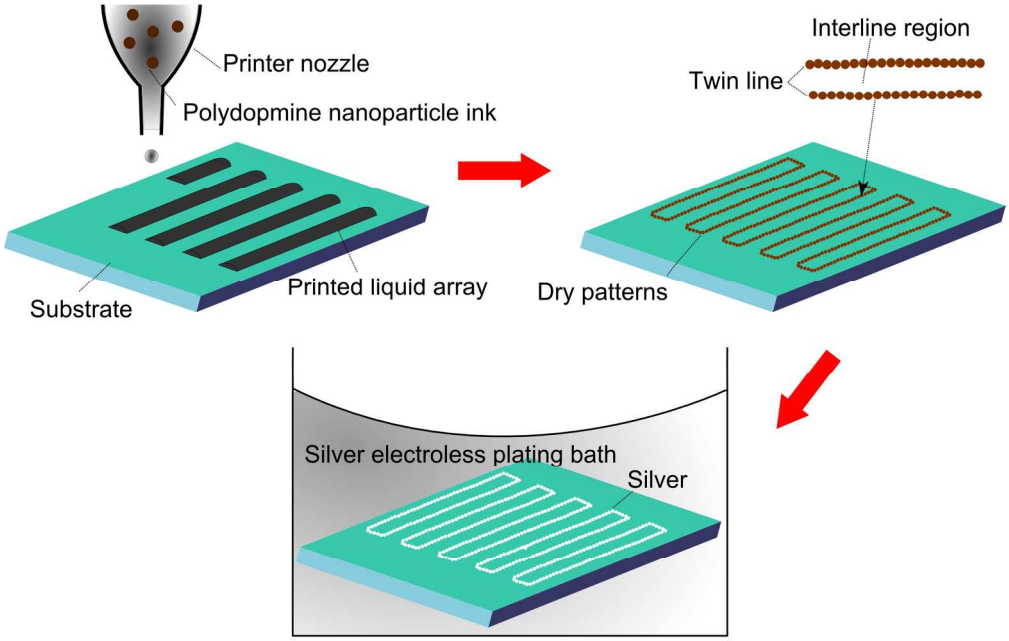

686x444mm (72 x 72 DPI)

Journal of Materials Chemistry C Accepted Manuscript